ELSEVIER

Chemical Engineering Journal 126 (2007) 131–138

Chemical Engineering Journal

www.elsevier.com/locate/cej

A comparison of collision kernels for sprays from one and two-nozzle atomisation systems

T.A.G. Langrish *, K. Kota

School of Chemical and Biomolecular Engineering, The University of Sydney, NSW 2006, Australia

Received 5 May 2005; received in revised form 12 July 2006; accepted 12 July 2006

Abstract

A comparison has been carried out of the use of two combinations of collision kernels to predict the coalescence rates in water sprays from a single nozzle and two nozzles together, based on measurements of droplet size distributions. In the single-nozzle case, combinations of parameters were fitted to experimental data to give a standard error for the difference between actual and fitted volume percentages in the final spray of 1.4% for the first kernel, while fitting the kernel of Abrahamson [J. Abrahamson, Collision rates of small particles in a vigorously turbulent fluid, Chem. Eng. Sci. 30 (11) (1975) 1371–1379] by similarly adjusting parameters gave a standard error of 0.68%. Using these fitted values of parameters with data from two nozzles together gave a standard error of 3.3% with the first kernel, compared with 2.2% for the kernel of Abrahamson [J. Abrahamson, Collision rates of small particles in a vigorously turbulent fluid, Chem. Eng. Sci. 30 (11) (1975) 1371–1379]. The relevance of the work is that the kernel of Abrahamson [J. Abrahamson, Collision rates of small particles in a vigorously turbulent fluid, Chem. Eng. Sci. 30 (11) (1975) 1371–1379] may be useful for these simple simulations and for computational fluid dynamics (CFD) simulations of coalescence and agglomeration in spray dryers that are based on Eulerian–Eulerian approaches.

Keywords: Collision kernels; Coalescence; Agglomeration; Sprays

1. Introduction

Spray drying involves converting a liquid feedstock into dried particulate solids or powders in a drying chamber. A solution, an emulsion, a suspension, or slurry, is dispersed as a feedstock in a stream of hot gas as a spray, where dried particulate solids are produced by the evaporation of moisture. Drying occurs very rapidly because the feedstock is atomised into small droplets, which give a large surface area for evaporation and lead to high evaporation rates. In addition, the temperature of the drying particles is constrained by evaporative cooling, preventing product overheating while allowing relatively high inlet-air temperatures for rapid drying. Faster drying at lower temperatures improves thermal economy, minimises heat damage for heat-sensitive materials, and in the case of foodstuffs, reduces losses in flavour and aroma.

The dairy industry in New Zealand and Australia uses spray drying extensively to produce powdered-milk products. The dairy industry in Australia produces hundreds of thousands of tonnes of skim-milk powder each year for export, and in New Zealand the production of milk powder is a multi-billion dollar export industry. Any improvement in spray-drying technology or operation could result in major financial benefits to both countries. Internationally, spray drying is widely used to produce detergents, paint pigments, and many other consumer products. The primary aim in drying milk powders is to remove moisture from the materials with the minimum of heat damage and maximum efficiency. Another aim is to control the bulk density and to improve the dissolution, wetting, dispersing, and flow properties of the product by agglomerating the fine particles to produce coarser particles. This is especially important in the production of coarse spray-dried milk powders with "instant" properties, enabling rapid dissolution of the powders. During the spray-drying process, agglomerates can form on the walls or by coalescence in the bulk of the dryer chamber. Many studies [2–5] have focused on coalescence of droplets with nozzle sprays in simple geometries like single stand-alone sprays.

* Corresponding author. Tel.: +61 2 9351 4568; fax: +61 2 9351 2854.
E-mail addresses: tim.langrish@usyd.edu.au, timl@chem.eng.usyd.edu.au (T.A.G. Langrish), kkota@chem.eng.usyd.edu.au (K. Kota).

1385-8947/$ – see front matter © 2006 Elsevier B.V. All rights reserved.
doi:10.1016/j.cej.2006.07.015

The occurrence of coalescence and its outcomes in terms of powder properties are affected by many factors. These factors include the dryer configuration, the operating conditions within the dryer such as the temperature and humidity, the particle size distribution generated by the atomiser, and the degree of mixing due to swirl and turbulence. In industrial spray drying, the agglomeration rate may be enhanced by pointing atomisers towards each other to force droplet or particle interaction, and by introducing fine particles in the region of the atomisers to increase the likelihood of collisions among particles and droplets. Prior to the final design of spray dryer, small-scale experimental tests are generally required to specify process conditions for a given application. The process conditions are then typically fine-tuned by trial and error during subsequent operation of the spray dryer because coalescence and drying kinetics are not properly understood. However, recent advances in computer power and techniques have allowed the use of computational fluid dynamics (CFD) methods to model the transport phenomena within a spray dryer with relative ease compared with empirical techniques. CFD has the potential to become a powerful tool in spray-dryer design and optimisation. However, the computational requirements for coalescence simulations within CFD are considerable [6], so there is a motivation for investigating a simpler approach to coalescence simulations.

Such a simpler approach is investigated in this work, and this approach gives some insight into resolving the question of whether relative velocity or turbulence is more important in affecting collision rates between particles or droplets in gases. The simulation of sprays is important for many spray-drying applications in environmental engineering, such as flue gas desulphurization, and in many environmental situations including droplets, such as in clouds.

2. Agglomeration simulations

Where there is a differential velocity amongst droplets in a gas, so that the droplets are able to approach each other, the droplets may collide and coalesce or agglomerate. This relative movement can occur due to the turbulent motion of the fluid and differences in spray inertia due to the presence of a distribution of droplet sizes and velocities.

2.1. Theory

Fig. 1 shows a droplet with diameter d travelling at a relative velocity u_r though a field of droplets. The product of the effective cross-section of the droplet and the relative velocity gives the volume swept out by this droplet per unit time, as follows:

$$\dot{V} = \frac{\pi}{4} d^2 u_r \tag{1}$$

Assuming that the droplet collides and agglomerates with every other droplet in the volume swept out along the flight path, then the agglomeration rate is simply equal to the number density of droplets (number per unit volume) multiplied by the swept out volume per unit time,

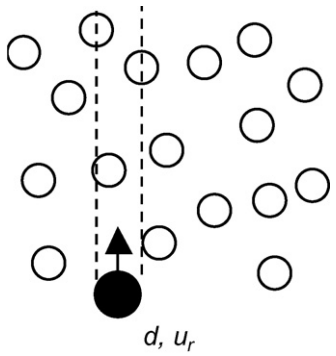

Fig. 1. Schematic diagram showing a droplet sweeping out a volume of the surrounding fluid, including other droplets.

$$\dot{W} = n\dot{V} \tag{2}$$

The total number of collisions, accounting for every droplet in the flow, is equal to the number of collisions for one droplet $\dot{W} = n\dot{V}$ multiplied by the total number of droplets per unit volume n. A factor of one-half must be included to ensure that each collision of two droplets is counted only once:

$$\dot{J} = \frac{1}{2} n^2 \left(\frac{\pi}{4} d^2\right) u_r \tag{3}$$

Eq. (3) is applicable to mono-disperse droplet clouds with relative velocities occurring among the similar sized droplets due to the eddying motion of the fluid, although it can be extended to account for droplets of different sizes, concentrations, and velocities. An efficiency factor can be included in Eq. (3) to account for droplets that do not successfully collide and agglomerate. Beard and Ochs [7] have shown that this efficiency lies between 50 and 100% for agglomeration between two droplets from very different size classes, one 10–30 μm in diameter and the other water droplet 50–500 μm in diameter.

From Kolmogorov's theory of isotropic turbulence, the relative velocity between droplets is given by the expression [8]:

$$u_r = \left(\frac{1}{15}\right)^{1/2} \left(\frac{\varepsilon}{\nu}\right)^{1/2} d \tag{4}$$

Here it is assumed that the diameter of the droplet is much smaller than Kolmogorov's micro-scale of the turbulence, given by the expression

$$\lambda = \left(\frac{\nu^3}{\varepsilon}\right)^{1/4} \tag{5}$$

The rate of turbulent energy dissipation is ε ($m^2\,s^{-3}$), and ν is the kinematic viscosity of the fluid ($m^2\,s^{-1}$). Kolmogorov's micro-scale is greater than 100 μm everywhere in many turbulent sprays. This value is estimated from CFD predictions for the rate of turbulent energy dissipation within a spray, which never exceeds 1 $m^2\,s^{-3}$ [6]. Thus, Eq. (4) is an appropriate expression for the relative velocity of droplets in isotropic turbulence, given that droplets within spray dryers are often less than 100 μm.

The relative velocity (different inertia between droplets) measured between droplets of different size close to the nozzle is

between 1 and 10 m s^{-1}. This is between 1000 and 10,000 times greater than the relative velocity due to the turbulent nature of the flow. Therefore, collisions due to differences in inertia between droplets are considerably more likely than collisions due to turbulence. Vohl et al. [9] have increased the rate of collisions between different-sized droplets within a wind tunnel by 10% when switching from a laminar flow to a turbulent flow. This suggests that although turbulence can enhance the rate of agglomeration, inertial effects remain the dominant mechanism.

For two groups of unequal sized droplets, the number of collisions of a droplet in size class i with droplets in size class j is $n_j\dot{V}$. Thus, the total number of collisions of droplets in size class i with droplets in size class j is $1/2 n_i n_j \dot{V}$. The swept out volume is based on the average droplet diameter. Hence, the collision rate is given by the expression

$$\dot{J}_{ij} = \frac{1}{2} n_i n_j \frac{\pi}{4} \left[\frac{d_i + d_j}{2}\right]^2 u_r \tag{6}$$

2.1.1. Collisions due to eddying motion (turbulence)

For each size class within the distribution of droplet sizes, Eq. (3) may be applied. The kinematic viscosity of air is 10^{-5} m^2 s^{-1}. The turbulent energy dissipation rate is no more than 1 m^2 s^{-3}. From Eq. (4), the relative velocity of droplets due to turbulence is of order $u_r = (1/15)^{0.5} \times (1/10^{-5})^{0.5} \times d_p \approx (1/15)^{0.5} \times (1/10^{-5})^{0.5} \times d_p$ m s^{-1}.

2.1.2. Collisions due to differential inertia

For collisions between different size classes, Eq. (6) may be applied.

2.1.3. Collisions due to turbulence and external forces

Abrahamson [1] used gas kinetic theory to predict collision rates in high-intensity turbulence produced when pumping suspensions. His suggested (full) collision rate expression is as follows:

$$\dot{J}_{ij} = 2^{3/2}\pi^{1/2} n_i n_j (d_i + d_j)^2 \sqrt{\overline{U_{P_i}^2} + \overline{U_{P_j}^2}} \times \exp\left[-\frac{u_r^2}{2(\overline{U_{P_i}^2} + \overline{U_{P_j}^2})}\right] + \pi n_i n_j (d_i + d_j)^2 \times \frac{u_r^2 + \overline{U_{P_i}^2} + \overline{U_{P_j}^2}}{u_r} \operatorname{erf}\left[\frac{u_r}{\sqrt{2(\overline{U_{P_i}^2} + \overline{U_{P_j}^2})}}\right] \tag{7}$$

Here $\overline{U_{P_i}^2}$ and $\overline{U_{P_j}^2}$ are the fluctuating velocities for droplets i and j, respectively. This equation was shown to be equivalent to Eq. (6) in the case of no turbulence. The fluctuating velocities for the droplets are related to the fluctuating velocity for the gas ($\overline{U^2}$) by the equation [1]:

$$\overline{U_P^2} = \frac{\overline{U^2}}{1 + 1.5\tau_p \varepsilon / \overline{U^2}} \tag{8}$$

The fluctuating velocity for the gas may be estimated from the mean gas velocity (u_{gas}) using the turbulence intensity (TI), from the following equation:

$$\overline{U^2} \approx (\mathrm{TI} u_{gas})^2 \tag{9}$$

2.2. Procedure

The purpose of these simulations is to assess if the amount of coalescence measured in a region starting some distance away from the atomiser can be predicted by a simple simulation. The distance from the nozzle at the start of the region is d_1, and the distance from the nozzle at the end of the region is d_2.

The overall region for the coalescence simulations is split into a number of subdivisions, with volume V for each subdivision. The total volumetric flow rate (Q) entering each subdivision is conserved. The distance increment for each subdivision is denoted by Δd.

At the inlet of the first subdivision, the total volumetric flow rate is split between each droplet size according to the volumetric droplet size distribution (V_i) assessed by the Malvern size analyser, resulting in a volumetric flow rate for each droplet size (Q_i). Then, by dividing by the volume of each droplet size, the number flow rate (N_i, number s^{-1}) for each droplet size (d_{p_i}) entering the first subdivision can be assessed.

$$Q_i = V_i Q \tag{10}$$

$$N_i = \frac{Q_i}{\pi/6 d_{p_i}^3} \tag{11}$$

The droplet residence time (τ_i) for each droplet size is calculated by integrating the changing droplet velocity (u_p) over the distance increment for each subdivision (Δd) from the start to the end of the subdivision, so that:

$$\tau_i = \int_0^{\Delta d} \frac{\mathrm{d}x}{u_{p_i}} \qquad u_{p_i} = \frac{\mathrm{d}x(\text{for particle size } i)}{\mathrm{d}t} \tag{12}$$

The droplet velocity for each size class (u_{p_i}) follows an unsteady-state force balance equation, assuming that the inertial deceleration is caused only by the drag force for the horizontal jet (hence ignoring the effects of gravity):

$$m_{p_i}\frac{\mathrm{d}u_{p_i}}{\mathrm{d}t} = \rho_p \frac{\pi}{6} d_{p_i}^3 \frac{\mathrm{d}u_{p_i}}{\mathrm{d}t} = -C_{D_i}\frac{1}{2}\rho(u_{p_i} - u_g)^2 \frac{\pi}{4} d_{p_i}^2 \frac{\mathrm{d}u_{p_i}}{\mathrm{d}t} = -C_{D_i}\frac{3}{4}\frac{\rho}{\rho_p}\frac{(u_{p_i} - u_g)^2}{d_{p_i}} \tag{13}$$

Here m_{p_i} is the droplet mass for each size class, ρ the fluid (air) density (1.2 kg m^{-3} at 20 °C), ρ_p the droplet (water) density (1000 kg m^{-3} at 20 °C), u_g the gas velocity (m s^{-1}), and C_{D_i} is the drag coefficient, given by Stokes law ($C_{D_i} = 24/Re_{p_i}$) for low Reynolds numbers ($Re_{p_i} < 0.3$) and by the Schiller–Naumann Eq. [10] for intermediate droplet Reynolds

numbers ($0.3 < Re_{p_i} < 500$):

$$C_{D_i} = \frac{24}{Re_{p_i}}(1 + 0.15 Re_{p_i}^{0.687}) \quad (14)$$

$$Re_{p_i} = \frac{\rho |u_{p_i} - u_g| d_{p_i}}{\mu} \quad (15)$$

where μ is the dynamic viscosity of the air (1.8×10^{-5} kg m^{-1} s^{-1} at 20 °C).

The initial velocity of every droplet size is assumed to be the same. All droplets are assumed to have the same density, and it is assumed that all droplets are distributed evenly over the control volume.

The number concentration (n_i, number per unit volume) that is required in Eqs. (3) and (6), or Eq. (7), for the collision rates can then be estimated from the number flow rate of each droplet size into the subdivision (N_i) multiplied by the residence time (τ_i) of that droplet size divided by the volume of the subdivision (V).

$$n_i = \frac{N_i \tau_i}{V} \quad (16)$$

Then, between each pair of droplet size classes i and j for the whole range of droplets, Eqs. (3) and (6), or Eq. (7), are used to predict the collision rates (numbers per unit volume per unit time), J_{ij}. In using these equations, information on the turbulent energy dissipation rates in the subdivision are necessary. The number of collisions (per unit volume) between droplet size classes i and j within this subdivision are estimated from:

$$n_{coll_{ij}} = J_{ij} \min(\tau_i, \tau_j) \quad (17)$$

The number of collisions is estimated as the product of the collision rate and the minimum residence time of the two classes of droplets in the control volume. Each value of $n_{coll_{ij}}$ can correspond to a loss of volume (Δvol_{ij}) from droplet size classes i and j. This loss of droplet volume (per unit volume within the subdivision) is equal to $n_{coll_{ij}} \pi/6 d_{p_i}^3$ for size class i and $n_{coll_{ij}} \pi/6 d_{p_j}^3$ for size class j (for collisions between droplet size classes i and j) or $2 n_{coll_{ij}} \pi/6 d_{p_i}^3$ for collisions between droplet size class i and itself.

The corresponding gain in droplet volume (per unit volume within the subdivision, Δvol_{ij}) occurs for the droplet size class that is closest to the coalesced droplet. Assuming that these water droplets remain spherical, this new droplet diameter is equal to $(2 d_{p_i}^3)^{1/3}$ for collisions between droplet size class i and itself or $(d_{p_i}^3 + d_{p_j}^3)^{1/3}$ for collisions between droplet size classes i and j.

The next step is to find the closest diameter to this new size, denoted by d_{p_k} and increase the number concentration (droplets per unit volume) in this size class by $\Delta vol_{ij}/\pi/6 d_{p_k}^3$.

After the new number concentrations (n_i, number per unit volume) have been obtained, the number flow rate of each droplet size out of the subdivision (N_i) may be estimated from the new number concentrations (n_i) multiplied by the volume of the subdivision (V) divided by the residence time (τ_i) of that droplet size.

$$N_i = \frac{n_i V}{\tau_i} \quad (18)$$

The number flow rate of each droplet size out of the subdivision (N_i) then becomes the number flow rate of each droplet size into the next subdivision.

An implicit assumption in this simulation procedure is that new, coalesced, droplets have the same velocity and residence time as the droplets in the class into which they fall, so this procedure does not carry out the momentum balance calculations that would be necessary to calculate the new velocities.

3. Materials and methods

The nozzles were low flow rate two-fluid ones from the manufacturer BETE, model number 1/4″ XA00SR050A, atomising water with air with external mixing and a maximum flowrate of 2 l h^{-1} at an air atomising pressure of 4 bar gauge for a siphon-fed system. Sets of coalescence data from Valencia-Bejarano [11] and Valencia-Bejarano and Langrish [12] have been used as a base case. The simulations for one nozzle have been carried

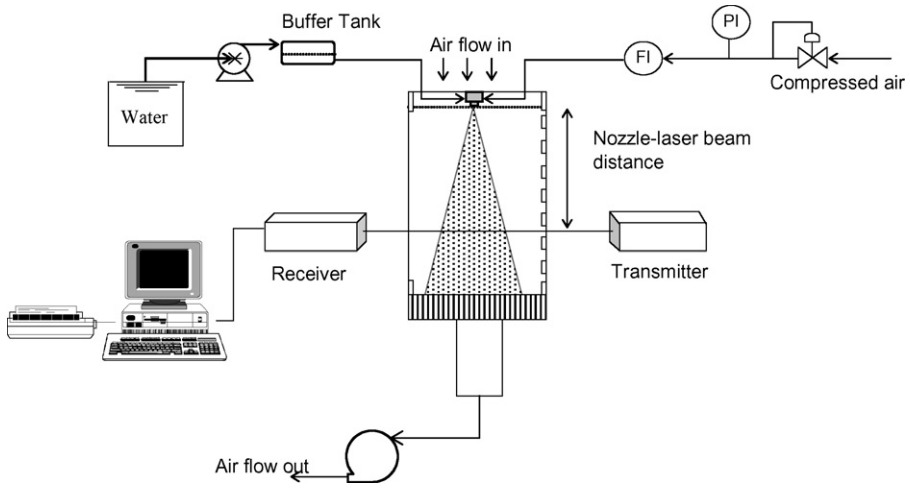

Fig. 2. Schematic diagram of the experimental equipment used for the one-nozzle case [12].

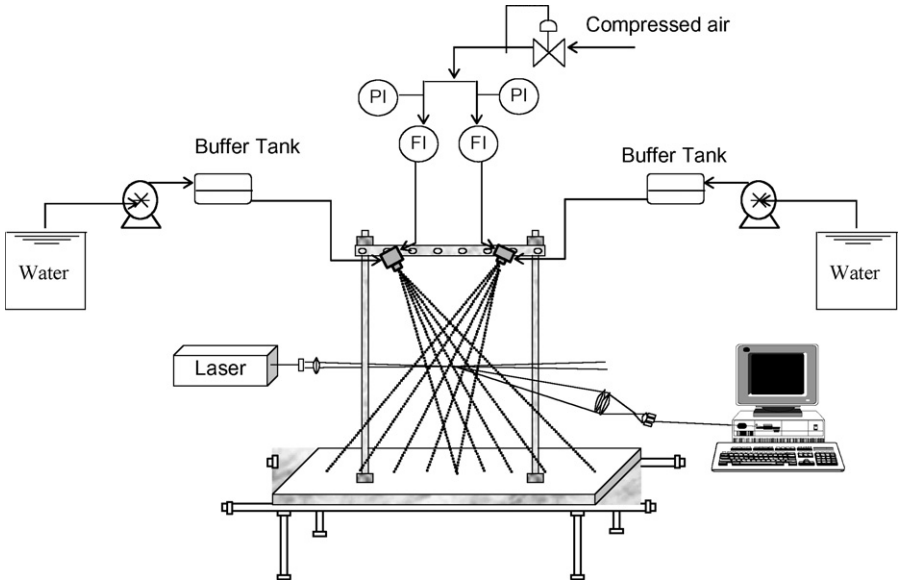

Fig. 3. Schematic diagram of the experimental equipment used for the two-nozzle case [11].

out between the two axial locations downstream of the nozzle, 45 and 245 mm from the nozzle outlet. The apparatus (Fig. 2) is described in more detail by Valencia-Bejarano and Langrish [12], while that for the two-nozzle case is described by Valencia-Bejarano [11]. For the two-nozzle case, the outlets of the nozzles were 45 mm apart, and the nozzles were directed towards each other at an angle of 45° to the vertical direction. For the simulations, 200 equally sized subdivisions in the direction along the spray were found to give a grid-independent solution (Fig. 3).

4. Results and discussion

4.1. Single-nozzle case

4.1.1. Individual contributions to coalescence kernel

For the individual coalescence kernels, Eqs. (3) and (6), a reasonable fit of the actual and predicted final droplet size distributions (a standard error of 1.4% for the percentages in the droplet sizes) can be obtained with the following values for the parameters, as shown in Fig. 4:

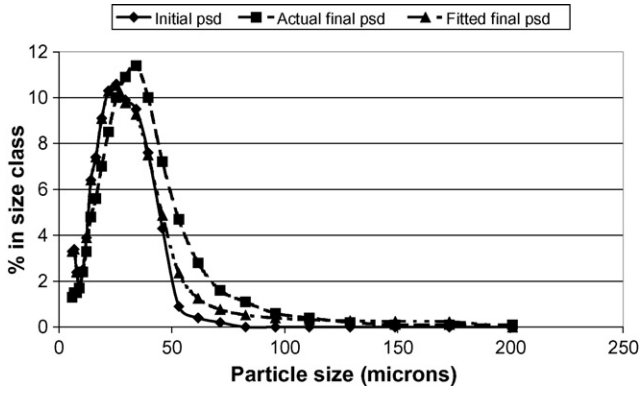

Fig. 4. Initial and final droplet size distributions for the base case, comparing the fitted and actual final droplet size distributions.

- a gas velocity (u_g) of 7.54 m s^{-1};
- an initial droplet velocity (u_{p_i}) of 12 m s^{-1};
- an energy dissipation rate (ε) of 1 m^2 s^{-3};
- a liquid flowrate (Q_l) of 16.7 ml min^{-1};
- a jet angle (θ) of 20°;
- an initial jet diameter ($d_{jetinit}$) of 1 mm.

The initial droplet velocity has been measured using phase-doppler particle anemometry and reported by Nijdam et al. [13]. As mentioned in Section 2, the turbulent energy dissipation rate is around 1 m^2 s^{-3} in the spray. The liquid flow rate is the actual measured value. The manufacturer states the jet angle to be between 17° and 22°, and estimates of the actual jet angle suggest that this is a reasonable estimate. The jet opening is between 0.8 and 1.5 mm in actual diameter. The gas velocity was not measured, and so was the main fitted parameter, as guided by the sensitivity analysis shown in Table 1, which gives the impact of possible changes in model parameters on the final predicted mean diameter.

In terms of the actual and fitted average final droplet sizes, the actual average was 30.8 μm, while the fitted average was 28.8 μm (Table 1). While the air velocity and the energy dissipation rate (ε) are not completely independent, the lack of significant sensitivity for the mean diameter in Table 1 to a value for the energy dissipation rate that is two orders of magnitude different to the base case suggests that, in this case, the effects of turbulence and collisions due to eddying motion are small. Most of the coalescence must therefore be caused by the relative motion of droplets, which can be appreciated by the very different slip, or relative, velocities between the droplets and the gas (0.003 m s^{-1} for 10 μm droplets, 0.07 m s^{-1} for 50 μm droplets) and therefore each other. In Table 1, the parameters having the greatest impact are the gas and liquid velocities, pointing to the relative velocity between droplets as having the greatest impact on coalescence rates. The effects of jet angle and liquid flow rate,

Table 1
The impact of possible changes in model parameters on the average final droplet sizes

	Average final droplet size (μm)
Base case $u_g = 7.54\ m\ s^{-1}$, $u_{p_i} = 12\ m\ s^{-1}$ $\varepsilon = 1\ m^2\ s^{-3}$ $Q_l = 16.7\ ml\ min^{-1}$ $\theta = 20^o$, $d_{jetinit} = 1\ mm$	28.8 (fitted) 30.8 (actual)
$u_g = 6\ m\ s^{-1}$	46.1 (+60% increase compared with the base case, fitted)
$u_g = 9\ m\ s^{-1}$	25.1 (−13%)
$u_{pi} = 10\ m\ s^{-1}$	25.3 (−12%)
$u_{pi} = 15\ m\ s^{-1}$	38.5 (34%)
$\varepsilon = 0.01\ m^2\ s^{-3}$	28.8 (0%)
$Q_l = 20\ ml\ min^{-1}$	31.9 (11%)
$\theta = 17^\circ$	35.5 (23%)
$\theta = 22^\circ$	26.9 (−7%)
$d_{jetinit} = 0.8\ mm$	29.1 (1%)
$d_{jetinit} = 1.5\ mm$	28.4 (−1%)

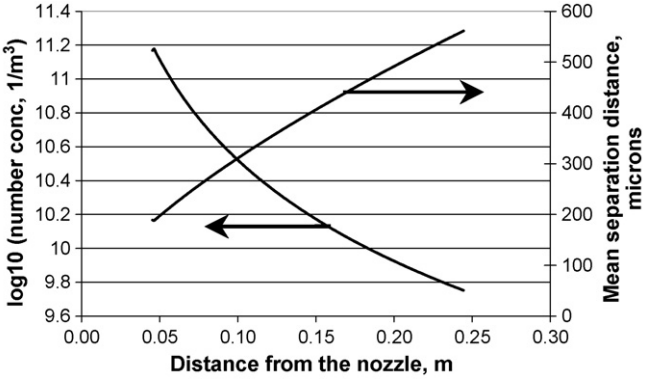

Fig. 5. Predicted number concentrations and mean separation distances (droplet to droplet) as a function of distance for the base case.

which affect the predicted droplet number concentration, are also significant. The predicted importance of the number concentration in affecting the coalescence process is also emphasised in Figs. 5 and 6. Here, the greatest rate of increase in the mean size occurs near to the nozzle, where number concentrations are over $10^{10.5}$ droplets m^{-3} and the mean separation distances for these

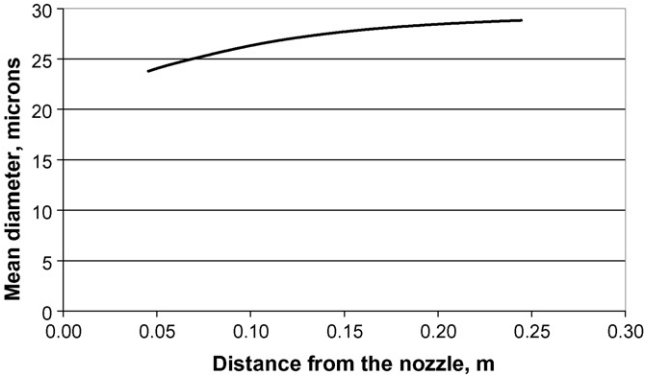

Fig. 6. Predicted mean diameter as a function of distance for the base case (corresponding to Fig. 3).

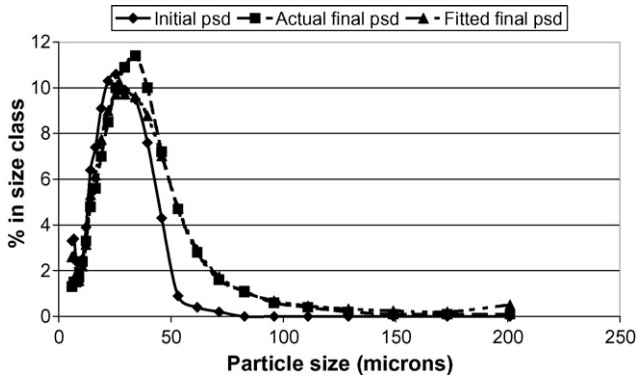

Fig. 7. Initial and final droplet size distributions for the base case, comparing the fitted and actual final droplet size distributions for the collision rate kernel of Abrahamson [1].

droplets, which range from 5 to 200 μm and average around 30 μm, are under 300 μm. Hence this simplified coalescence simulation gives considerable insight into the key parameters involved in the process, namely relative velocity and number concentration.

4.1.2. The collision rate kernel of Abrahamson

For the combined coalescence kernels [1], Eq. (7), a better fit of the actual and predicted final droplet size distributions (a standard error of 0.68% for the percentages in the droplet sizes) can be obtained with the following values for the parameters, as shown in Fig. 7:

- gas (u_g) and initial droplet (u_{p_i}) velocities, both of $12\ m\ s^{-1}$;
- an energy dissipation rate (ε) of $200\ m^2\ s^{-3}$;
- a turbulence intensity (TI) of 1.8%;
- a liquid flowrate (Q_l) of $16.7\ ml\ min^{-1}$;
- a jet angle (θ) of 20°;
- an initial jet diameter ($d_{jetinit}$) of 1 mm.

The energy dissipation rate is at the lower end of the range suggested by Abrahamson [1] for pipe flows. The gas velocity and the turbulence intensity were not measured, and so were the main fitted parameters. In the same way as with the previous kernel, a good fit can be achieved between the experimental data and the kernel by adjusting the above parameters. Table 2, like Table 1, shows that the greatest impacts come from the gas and liquid velocities, again indicating that the relative velocity between droplets has the greatest impact on coalescence rates. Turbulence is also very important, but not as significant as the relative velocities. In terms of the actual and fitted average final droplet sizes, the actual average was 30.8 μm, while the fitted average was 31.5 μm (Table 2). Physically, the effects of air velocity and hence number concentration are highly non-linear, since the collision rate is dependent on the number concentration squared. Reducing air velocity means a higher number concentration and hence a higher collision rate. The overall effect is even more non-linear than this, since the lower air velocity also means greater residence time in the spray, so both the collision rate and the time over which the collisions

Table 2
The impact of possible changes in model parameters on the average final droplet sizes for the collision rate kernel of Abrahamson [1]

	Average final droplet size (μm)
Base case $u_g = u_{p_i} = 12\,m\,s^{-1}$ $\varepsilon = 200\,m^2\,s^{-3}$ TI = 1.8%, $Q_l = 16.7\,ml\,min^{-1}$ $\theta = 20^\circ$, $d_{jetinit} = 1$ mm	31.5 (fitted) 30.8 (actual)
$u_g = 11.5\,m\,s^{-1}$	73.1 (+132% compared with the base case, fitted)
$\varepsilon = 500\,m^2\,s^{-3}$	29.7 (−6%)
TI = 2.5%	46.3 (47%)
$Q_l = 20\,ml\,min^{-1}$	34.2 (9%)
$\theta = 17^\circ$	37.2 (18%)
$\theta = 22^\circ$	29.5 (−6%)
$d_{jetinit} = 0.8$ mm	31.7 (1%)
$d_{jetinit} = 1.5$ mm	31.0 (−1%)

occur are greater when the air velocity is reduced. The effects of number concentration, collision rate and residence time are all included in the model, though Eqs. (6), (10)–(12), and (16)–(18). The likelihood of the effects being numerical artifacts is low, because a grid sensitivity test with the model shows no significant effect, with a 50% increase in the number of subdivisions (from 200 to 300) changing the average final droplet size by less than 0.2%. The difference between the standard errors of 3.3 and 0.68% is significant at the 95% confidence level, suggesting that the difference between fitting the two kernels is significant.

4.2. The two-nozzle case and overall discussion

For this case, the only parameter fitted to the data was the intersection distance from the nozzle, which was found to be 80 mm. This distance is within experimental uncertainties of the actual intersection point, which was virtually the same distance (±5 mm, given the width of the spray). The base case parameters from Tables 1 and 2 were used for the case of the first kernel used (Eqs. (3) and (6)) and the kernel of Abrahamson [1], respectively. In terms of the actual and fitted average final droplet sizes, the actual average was 39.1 μm, while the fitted average from the use of the first kernel was 39.7 μm and that from using the kernel of Abrahamson [1] was 41.1 μm.

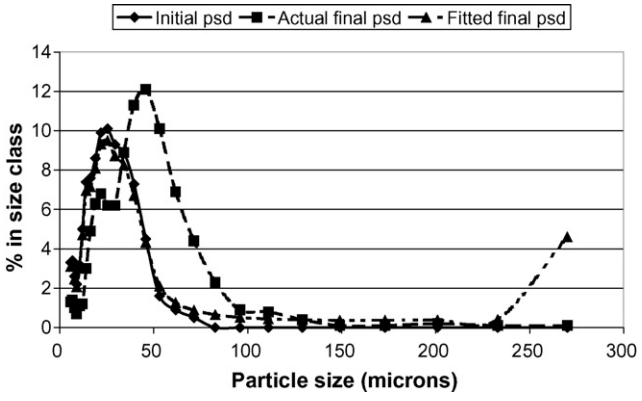

Fig. 8. Initial and final droplet size distributions for the two-nozzle case, comparing the fitted and actual final droplet size distributions.

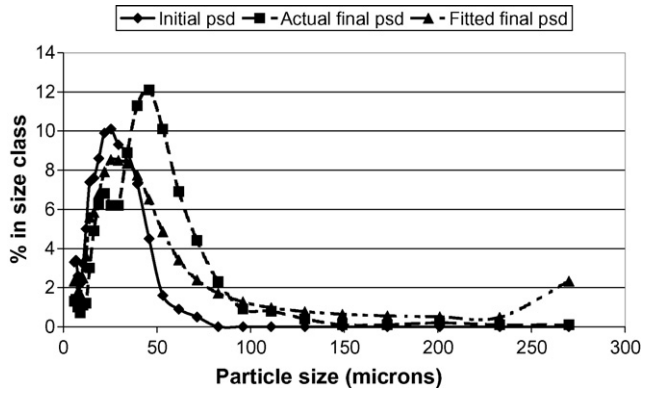

Fig. 9. Initial and final droplet size distributions for the two-nozzle case, comparing the fitted and actual final droplet size distributions with the collision rate kernel of Abrahamson [1].

Given that these distributions are not highly fitted in a direct sense, it is only natural that the degree of fit between the fitted and actual percentages in the droplet sizes is worse for this two-nozzle case than the single-nozzle one. For the first kernel, the standard error was 3.3% for the two-nozzle case (Fig. 8) compared with 1.4% for the single-nozzle case, while for the kernel of Abrahamson [1], the standard error was 2.2% for the two-nozzle case (Fig. 9) compared with 0.68% for the single-nozzle case. As with the single-nozzle case, neither kernel is particularly good for small droplets of 50 μm or under. However, the kernel of Abrahamson [1] is noticeably better for larger droplets.

This conclusion regarding the strength of the kernel of Abrahamson [1] is potentially useful for these simple simulations and for CFD simulations of coalescence and agglomeration in spray dryers that are based on Eulerian–Eulerian approaches, with the droplet phase being treated as a continuum. However, Nijdam et al. [6] suggest that Eulerian–Eulerian approaches to CFD simulations of coalescence and agglomeration in spray dryers are intrinsically more difficult than Eulerian–Lagrangian treatments, where the droplet phase is treated as set of discrete representative droplets. Nevertheless, the approach taken in this paper involving the use of a collision kernel for Eulerian–Eulerian type simulations of aggregation and agglomeration has been used in the literature, for example, by Hounslow et al. [14] and Zuev and Lepeshinskii [15].

5. Conclusions

The standard error from fitting parameters to experimental data for a single spray was 1.4% for the first kernel. Fitting the kernel of Abrahamson [1] by similarly adjusting parameters gave a standard error of 0.68%. For the first kernel and the two-nozzle case, using these fitted values of parameters gave a standard error of 3.3%, compared with 2.2% for the kernel of Abrahamson [1]. The kernel of Abrahamson [1] is better than others for larger droplets and for these simple simulations, suggesting that it may be helpful for CFD simulations of coa-

lescence and agglomeration in spray dryers that are based on Eulerian–Eulerian approaches.

Acknowledgements

Thanks are due to Dr. J. Nijdam for his work to derive the collision kernels and to the Australian Research Council for Large and Discovery Grant for funding this work.

References

[1] J. Abrahamson, Collision rates of small particles in a vigorously turbulent fluid, Chem. Eng. Sci. 30 (11) (1975) 1371–1379.
[2] M. Gavaises, A. Theodorakakos, G. Bergeles, G. Brenn, Evaluation of the effect of droplet collisions on spray mixing, J. Mech. Eng. Sci. Part C 210 (5) (1996) 465–475.
[3] Y. Hardalupas, J.H. Whitelaw, Interaction between sprays from multiple coaxial air blast atomizers, J. Fluids Eng. Trans. ASME 118 (4) (1996) 762–771.
[4] D.L. Bulzan, Y. Levy, S.K. Aggarwal, S. Chitre, Measurements and predictions of a liquid spray from an air-assist nozzle, Atomization Sprays 2 (4) (1992) 445–462.
[5] G. Brenn, F. Durst, A. Selbach, Experimental investigations of the binary interaction of polydisperse sprays, Part. Part. Syst. Char. 15 (6) (1998) 263–273.
[6] J.J. Nijdam, B. Guo, D.F. Fletcher, T.A.G. Langrish, Challenges of simulating droplet coalescence within a spray, Dry. Technol. Int. J. 22 (6) (2004) 1463–1488.
[7] K. Beard, H.T. Ochs, Collection and coalescence efficiencies for accretion, J. Geophys. Res. 89 (D5) (1984) 7165–7169.
[8] M.A. Delichatsios, R.F. Probstein, Coagulation in turbulent flow: theory and experiment, J. Colloid Interface Sci. 51 (3) (1975) 394–405.
[9] O. Vohl, K. Mitra, S.C. Wurzler, H.R. Pruppacher, A wind tunnel study of the effects of turbulence on the growth of cloud drops by collision and coalescence, J. Atmos. Sci. 56 (24) (1999) 4088–4099.
[10] L. Schiller, A. Naumann, Über die grundlegenden Berechnungen der Schwerkraftaufbereitung (Fundamental calculations in gravitational processing), Z. Ver. Deut. Ing. 77 (1933) 318–320.
[11] M. Valencia-Bejarano, Experimental investigation of droplet coalescence in a poly-disperse full-cone spray, Master of Engineering (Research) Thesis, Department of Chemical Engineering, The University of Sydney, 2003.
[12] M. Valencia-Bejarano, T.A.G. Langrish, Experimental investigation of droplet coalescence in a full-cone spray from a two-fluid nozzle using laser diffraction measurements, Atomization Sprays 14 (4) (2004) 355–374.
[13] J.J. Nijdam, B. Guo, M. Valencia-Bejarano, T.A.G. Langrish, An experimental investigation of agglomeration with one and two nozzle atomization, Chin. J. Chem. Eng. 12 (6) (2004) 750–755.
[14] M.J. Hounslow, R.L. Ryall, V.R. Marshall, A discretized population balance for nucleation, growth, and aggregation, AIChE J. 34 (11) (1988) 1821–1824.
[15] Y.V. Zuev, I.A. Lepeshinskii, Two-phase multi-component turbulent jet with phase transitions, Fluid Dyn. 30 (5) (1995) 750–757.